Palaeogeography, Palaeoclimatology, Palaeoecology 527 (2019) 1–13

Contents lists available at ScienceDirect

Palaeogeography, Palaeoclimatology, Palaeoecology

journal homepage: www.elsevier.com/locate/palaeo

The relationship between leaf physiognomy and climate based on a large modern dataset: Implications for palaeoclimate reconstructions in China

Wen-Yun Chen[a,*], Tao Su[b], Lin-Bo Jia[c], Zhe-Kun Zhou[c,*]

[a] Department of Economic Plants and Biotechnology, Yunnan Key Laboratory for Wild Plant Resources, Kunming Institute of Botany, Chinese Academy of Sciences, Kunming 650201, China
[b] CAS Key laboratory of Tropical Forest Ecology, Xishuangbanna Tropical Botanical Garden, Chinese Academy of Sciences, Mengla 666303, China
[c] Key Laboratory for Plant Diversity and Biogeography of East Asia, Kunming Institute of Botany, Chinese Academy of Sciences, Kunming 650201, China

ARTICLE INFO

Keywords:
Dicot trees
Distribution pattern
Asian Monsoon
Multivariate statistics
Precipitation
Temperature

ABSTRACT

In this paper, correlation between modern leaf physiognomy and climate in China are examined, to optimize the use of leaf characters as a palaeoclimate proxy. A large dataset was compiled, recording the distribution of leaf physiognomic characters among 3166 native dicot trees species across 732 calibration grids on a county level. Grids span a range of ecological environments (tropical rainforests to alpine shrubs) across humid areas. Thirteen climatic parameters were included for each grid and 22 leaf physiognomic characters were scored for each tree species. The correlation between leaf physiognomic characters and climatic parameters were calculated based on single linear regressions (SLR) and multiple linear regressions (MLR). Results indicate clear spatial distribution patterns, linked to latitude, exist for all leaf characters, with temperature (Coldest Month Mean Temperature, CMMT) and precipitation (Growing Season Precipitation, GSP) being the main climate controls. Moreover, because leaf characters are more closely correlated with Precipitation during the Three Wettest Consecutive Months (P3WET), rather than with Precipitation during the Three Driest Consecutive Months (P3DRY), seasonal variations in rainfall associated with the Asian Monsoon might especially influence leaf physiognomic characters. Closer correlations between leaf physiognomy and climate are seen using MLR compared with SLR; therefore Mean Annual Temperature (MAT) and Mean Annual Precipitation (MAP) based on MLR equations provide the most promising basis for palaeoclimate reconstructions in China.

1. Introduction

Morphological characteristics of plants reflect functional adaptations that contribute to the optimization of physiological and ecological processes, thereby making them sensitive indicators of local climate. Leaf physiognomic characters of woody dicotyledons have been shown to have a strong correlation with climate in the majority of regions across the world (Bailey and Sinnott, 1915, 1916; Givnish, 1984; Wolfe, 1993; Wilf, 1997; Jacobs, 1999; Traiser et al., 2005; Royer and Wilf, 2006; Peppe et al., 2011; Yang et al., 2015; Wright et al., 2017). This leaf physiognomy-climate correlation has therefore been extensively used by palaeobotanists to develop proxies for reconstructing palaeoclimate (Wing and Greenwood, 1993; Wolfe, 1993; Kovach and Spicer, 1996; Wilf, 1997; Jacobs, 2002; Kowalski and Dilcher, 2003; Traiser et al., 2007; Peppe et al., 2011; Kennedy et al., 2014; Spicer et al., 2017).

Bailey and Sinnott (1915, 1916) initially suggested leaf physiognomy-climate correlations could be used to estimate palaeoclimate after recording a decline in the percentage of a flora with untoothed leaf margins correlating to a decline in temperature (with increasing latitude). Subsequently, palaeobotanists found that leaf physiognomic characters of modern dicot trees have a strong correlation with climate on regional, continental and global scales (Wolfe, 1979; Wing and Greenwood, 1993; Wilf et al., 1998; Jacobs, 1999; Gregory-Wodzicki, 2000; Greenwood et al., 2004; Traiser et al., 2005; Peppe et al., 2011; Yang et al., 2015; Wright et al., 2017). A large number of correlations have been proposed and widely used to qualitatively reconstruct palaeoclimate from Cretaceous to Cenozoic floras (Wolfe, 1979; Wing and Greenwood, 1993; Wilf et al., 1998; Jacobs, 1999; Gregory-Wodzicki, 2000; Greenwood et al., 2004; Traiser et al., 2007; Uhl et al., 2007; Peppe et al., 2011; Srivastava et al., 2012; Shukla et al., 2014; Herman et al., 2017; Bush et al., 2017; Ai et al., 2019). Although some factors, such as leaf life-span and historical genetic signals, have hampered palaeoclimate reconstructions (Jordan,

* Corresponding authors at: Kunming Institute of Botany, Chinese Academy of Sciences, 132# Lanhei Road, Kunming 650201, Yunnan, China.
E-mail addresses: chenwy@mail.kib.ac.cn (W.-Y. Chen), zhouzk@mail.kib.ac.cn (Z.-K. Zhou).

https://doi.org/10.1016/j.palaeo.2019.04.022
Received 27 December 2018; Received in revised form 10 April 2019; Accepted 24 April 2019
Available online 29 April 2019
0031-0182/

2011; Peppe et al., 2011; Royer et al., 2012), leaf physiognomy methods remain one of the most powerful and common tools to reconstruct terrestrial palaeoclimate (Bailey and Sinnott, 1916; Wing and Greenwood, 1993; Wilf, 1997; Peppe et al., 2011; Kennedy et al., 2014; Spicer et al., 2017).

Previous studies have used single univariate methods to analyze the relationship between a single climatic parameter and a single leaf physiognomic character (Wolfe, 1971, 1979, 1993; Dilcher, 1973; Givnish, 1984; Wing and Greenwood, 1993; Wilf, 1997; Jacobs, 1999; Gregory-Wodzicki, 2000; Greenwood et al., 2004; Malhado et al., 2009; Steart et al., 2010; Su et al., 2010; Chen et al., 2014; Li et al., 2016). Commonly applied methods include leaf-margin analysis (LMA) to estimate palaeotemperature (Wing and Greenwood, 1993; Kowalski, 2002; Greenwood et al., 2004; Miller et al., 2006; Peppe et al., 2011), and leaf-area analysis (LAA) to estimate palaeoprecipitation (Wilf et al., 1998; Jacobs, 1999; Greenwood et al., 2010; Sunderlin et al., 2011; Bush et al., 2017; Lowe et al., 2018). As several studies have observed that leaf physiognomy simultaneously integrates more characters that have a functional and/or physiological connection to climate (Wolfe, 1993; Kovach and Spicer, 1996; Wolfe and Spicer, 1999; Spicer et al., 2004, 2005; Royer et al., 2005, 2008; Traiser et al., 2005; Peppe et al., 2011; Kennedy et al., 2014; Yang et al., 2015), some investigations have therefore explored multivariate methods to synchronously analyze relationships between several leaf characters and climate. One such method is the Climate-Leaf Analysis Multivariate Program (CLAMP), which correlates 31 leaf characters and 11 climatic parameters. This method is a multivariate statistical method based on Canonical Correspondence Analysis (CCA) (Wolfe, 1993; Spicer, 2007, 2009, 2016; Spicer et al., 2005). Multiple linear regression models have also been developed using a dataset derived from the CLAMP calibration dataset or a comparable dataset using the CLAMP characters (Gregory, 1994; Stranks and England, 1997; Wiemann et al., 1998; Gregory-Wodzicki, 2000; Traiser et al., 2005; Lielke et al., 2012). Overall, palaeobotanists have explored multivariate methods that identify relationships among a variety of leaf characters and climatic variables simultaneously, and they have successfully applied these methods to reconstruct palaeoclimate (Herman and Spicer, 1996; Forest et al., 1999; Kennedy et al., 2002; Uhl et al., 2007; Godefroit et al., 2009; Tomsich et al., 2010; Srivastava et al., 2012; Shukla et al., 2014; Spicer et al., 2014; West et al., 2015; Herman et al., 2017; Ai et al., 2019).

Due to the wide range of climates and species distribution, large-scale datasets are important to aid our understanding of leaf physiognomy-climate relationships (Traiser et al., 2005; Kennedy et al., 2014; Yang et al., 2015; Wright et al., 2017). These datasets are difficult to compile using direct field sampling. Therefore, datasets including a large number of species and covering large areas are compiled to analyze leaf physiognomy-climate relationships using synthetic and chorological floras from previous publications. These datasets enable single/multiple transfer functions for climatic parameters to be calculated (Traiser et al., 2005). Using this approach makes it easy to explore distribution patterns of leaf physiognomy, and to analyze leaf physiognomy-climate correlations covering large areas which include a multitude of sampling sites. In addition, this method can reduce the influence of local factors on leaf physiognomy, such as edaphic conditions and microclimate factors (Traiser et al., 2005; Adams et al., 2008; Chen et al., 2014). Previous studies have demonstrated that this approach represents a promising tool for analyzing relationships between leaf physiognomy and climate (Traiser et al., 2005; Adams et al., 2008; Chen et al., 2014; Li et al., 2016).

The geographical extent of China covers a significant land area, ranging from tropical to cool temperate climates. As China also contains the majority of all major vegetation types in the world (Wu, 1980), it provides an ideal region to understand the spatial distribution of leaf physiognomy and the correlation between leaf physiognomy-climate, especially using a large dataset. Moreover, China experiences a strong Asian monsoon climate, characterized by wet summers and dry winters (Zhang, 1991). The modern Asian monsoon climate in China did not become established until the Paleogene (Spicer et al., 2017); the development of this monsoon climate may have been the main factor driving the evolution of the East Asian flora (Chen et al., 2018). Coupled with complex topography, these two factors contribute to southern China today hosting one of the world's great 'biodiversity hotspots' (Spicer, 2017; Spicer et al., 2017; Mosbrugger et al., 2018). To date, the study of leaf physiognomy-climate correlations in China have mainly focused on leaf margins and MAT (Su et al., 2010; Chen et al., 2014; Li et al., 2016), and datasets for CLAMP calibration (Jacques et al., 2011) with plot samples. These studies indicate distinctive relationships can be observed between leaf physiognomy and climate in China (Jacques et al., 2011; Su et al., 2013). However, these distinctive leaf physiognomic spectra need to be tested across a large scale.

In this study, we initially explore the distribution patterns of leaf physiognomic characters on a large scale in humid regions in China. Secondly, we investigate their correlations with climatic parameters. Thirdly, we develop multiple linear regression equations and analyze correlations between leaf characters and climatic parameters. MAT and MAP multiple linear transfer functions are then applied to test the availability of the two models for estimating temperature and precipitation.

2. Materials and methods

2.1. Dataset on species distribution

The focus of our investigation was humid regions in China, areas having a mean annual precipitation > 400 mm. Species distribution maps were obtained from the database of native woody dicotyledonous species in China. This dataset includes 3166 native woody species, belonging to 536 genera and 111 families (see the electronic Supplementary Data 1 of Chen et al., 2014). This dataset was derived from the *Seed Plant of China* (Wu and Ding, 1999), specimen records in the Herbarium of the Kunming Institute of Botany (KUN), and the *Flora of China* (Wu, 1979, 1980, 1982, 1984, 1988, 1995, 1996, 1998). Maps of the present-day distribution of 3166 species were compiled at county level and digitized for application in a Geographical Information System (GIS) (for more details on species distribution data see Chen et al., 2014). In our study, we restricted dataset to those counties which included at least 20 native woody species. This dataset has already been used to construct a palaeotemperature reconstruction model based on leaf-margin analysis (Chen et al., 2014). The geographic distribution of 732 calibration grids included in this analysis is shown in Fig. 1.

2.2. Leaf physiognomic data

In our study, each of the 3166 species characterized by 22 leaf physiognomic characters were scored in the analysis, including leaf lobe, leaf size, untoothed leaf margins, base of blade, apex of blade, leaf length-width ratios and shape of blade. Definitions of characters (Table 1) followed Ellis et al. (2009). Following the procedures of Wolfe (1993), values of 0 (character is absent) and 1 (character is present) were assigned to each leaf physiognomic character. Leaf physiognomic characters for each species were determined using specimens in the Herbarium of the Kunming Institute of Botany. For every species, three leaves from each specimen were randomly chosen to cover the range of each morphological character. Leaf physiognomic characters of each species are shown in Supplementary Data 1. The percentage of each leaf physiognomy species in each county was the sum of scores of all species divided by the number of all species included in the county. For each county the percentage of each leaf physiognomic character is shown in Supplementary Data 2.

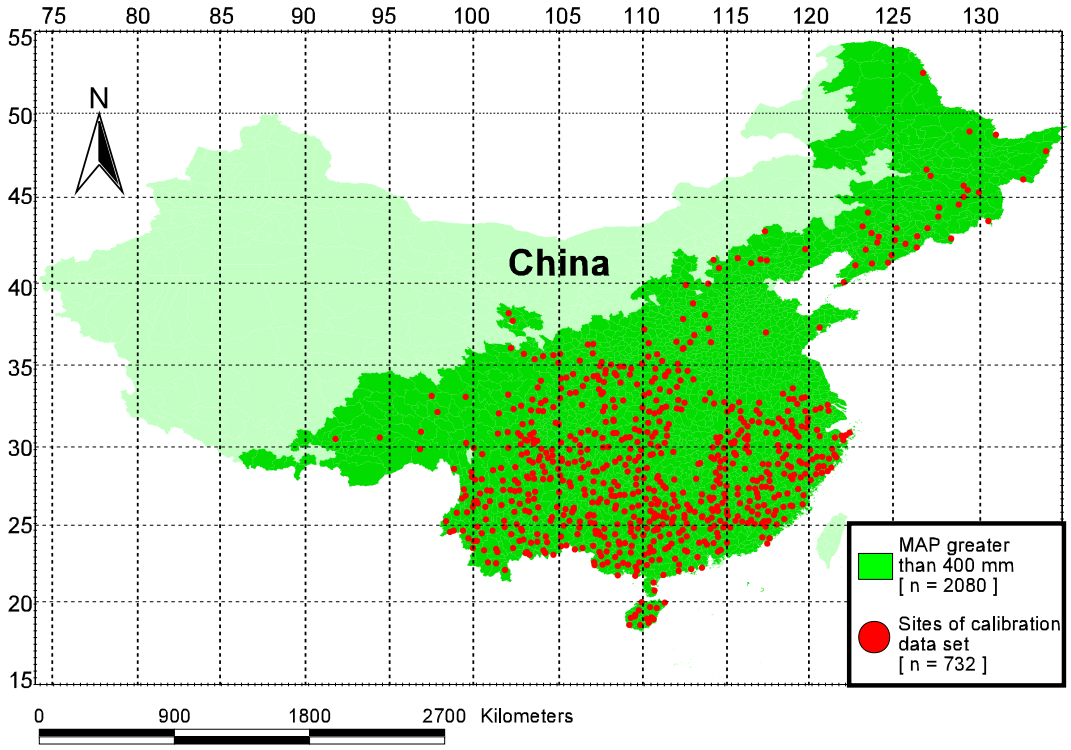

Fig. 1. Geographic distribution of calibration dataset. Grids with a minimum set of at least 20 species (sites of calibration dataset, n = 732).

2.3. Climatic parameters

Climate data with an average record of 30-years (1951–1980) were obtained from weather stations in each individual county with reference to Yunnan Provincial Meteorological Bureau (YPMB) and China Meteorological Data Sharing Service System (available online: http://cdc.cma.gov.cn/). Thirteen climatic parameters are included in this study: Mean Annual Temperature (MAT), Annual Temperature Sum (Tsum), Warmest Month Mean Temperature (WMMT), Coldest Month Mean Temperature (CMMT), Length of the Growing Season (GSL, months when the mean monthly minimum temperature exceeds 10 °C), Mean Annual Precipitation (MAP), Growing Season Precipitation (GSP), Mean Monthly Growing Season Precipitation (MMGSP), the Wettest Month Precipitation (Pmax), the Driest Month Precipitation (Pmin), Precipitation during Three Wettest Consecutive Months (P3WET), Precipitation during Three Driest Consecutive Months (P3DRY) and Relative Humidity (RH). These climatic parameters for each calibration grid are also shown in Supplementary Data 2.

2.4. Data analysis

The Chinese geographic patterns for the percentage of dicot trees in 21 leaf physiognomic characters were compiled and digitized for application using ARCVIEW (ArcView GIS 3.2, ESRI, New York, USA). All leaf characters were also plotted on a map at county level.

The relationships between the distribution patterns of the percentage of dicot trees of leaf physiognomic characters and geography (latitude and longitude) were quantified using single linear regressions (SLR).

To investigate the relationships between the percentage of leaf physiognomic characters and climatic parameters across the study area, SLR and multiple linear regressions (MLR) were applied. These regression models have been widely used to investigate correlations between leaf physiognomy and climate.

We calculated the correlation matrix between a single leaf physiognomic character and a single climatic parameter based on SLR, which set leaf physiognomy as the independent variable and climate as the dependent variable. The P-values of the correlation coefficients $<$ 0.01 were considered statistically significant. This correlation mainly consisted of climatic parameters which were predominantly controlling the geographic distribution of leaf physiognomic characters (Traiser et al., 2005; Chen et al., 2014). The MLR transfer functions were compiled using different climatic parameters to identify if leaf physiognomy synchronously integrated more characters coincidental with climate. In order to select the most outstanding leaf physiognomic characters in MLR, the 'forward stepwise regression' technique was used. This technique allowed the identification of four independent variables. The accuracy and precision of transfer functions were evaluated based on r^2 values and the standard error (SE) (Wing and Greenwood, 1993; Wiemann et al., 1998; Jacobs, 1999; Traiser et al., 2005; Peppe et al., 2011).

As MAT and MAP are widely estimated palaeoclimate parameters (Wing and Greenwood, 1993; Traiser et al., 2005; Peppe et al., 2011), we developed MAT and MAP transfer functions to test the availability of the two models for estimating temperature and precipitation.

All statistical analyses were conducted using SPSS 17 (SPSS Science, Chicago, IL, USA).

3. Results

3.1. Spatial distribution patterns of leaf physiognomic characters

The distribution patterns with the percentage of leaf physiognomic characters on Chinese woody dicotyledons show a clear geographical variable across the 732 calibration grids in humid regions in China (Figs. 2, 3 and S1; Table 2). Apart from leaf apex acute (ap_acut), other leaf physiognomies are more significantly correlated with latitude than longitude (Table 2). Among these leaf physiognomies that record a clear latitudinal trend, eleven leaf characters increase with an increase in latitude, including leaf lobe (le_lobe), nanophyll leaf size (ls_nano), microphyll leaf size (ls_micr), leaf apex obtuse (ap_obtu), leaf base obtuse (ba_obtu), leaf base reflex (ba_refl), leaf L: W ratio = 1–2:1

Table 1
Leaf physiognomic characters with minimum, maximum and mean percentages and ranges as they occur in the calibration dataset of 732 grids in humid regions in China. Definition of each leaf character follows the corresponding standard in the Manual of leaf architecture (Ellis et al., 2009).

	Leaf character	Abbr.	Definition	Min (%)	Max (%)	Mean (%)	Range (%)
1	Leaf simple	le_simp	Leaf is not compound	60.0	100.0	83.7	40.0
2	Leaf lobe	le_lobe	Leaf with lobes	0.0	33.3	4.2	33.3
3	Untoothed leaf margins	untooth	Margin without teeth	2.5	82.9	42.2	80.4
4	Leaf size: leptophyll	ls_lept	$< 25\ mm^2$	0.0	4.6	0.1	4.5
5	Leaf size: nanophyll	ls_nano	$25–225\ mm^2$	0.0	13.0	1.5	13.0
6	Leaf size: microphyll	ls_micr	$225–2025\ mm^2$	7.4	80.0	41.8	72.6
7	Leaf size: notophyll	ls_noto	$2025–4500\ mm^2$	9.7	61.9	35.4	52.5
8	Leaf size: mesophyll	ls_meso	$4500–18{,}225\ mm^2$	0.0	48.8	20.6	48.8
9	Apex of blade: obtuse	ap_obtu	$a > 90^0$	0.0	20.8	5.2	20.8
10	Apex of blade: acute	ap_acut	$a < 90^0$	75.6	100.0	93.7	24.4
11	Apex of blade: reflex	ap_refl	$a > 180^0$	0.0	12.2	1.0	12.2
12	Base of blade: obtuse	ba_obtu	$a > 90^0$	3.6	57.1	23.2	53.5
13	Base of blade: acute	ba_acut	$a < 90^0$	20.0	92.9	63.3	72.9
14	Base of blade: reflex	ba_refl	$a > 180^0$	0.0	52.2	13.5	52.2
15	Blade length: width < 1:1	lw_1	Ratio L/W: < 1:1	0.0	10.0	1.6	10.0
16	Blade length: width = 1–2:1	lw_2	Ratio L/W: = 1–2:1	0.0	68.2	25.7	68.2
17	Blade length: width = 2–3:1	lw_3	Ratio L/W: = 2–3:1	12.5	68.0	47.4	55.5
18	Blade length: width = 3–4:1	lw_4	Ratio L/W: = 3–4:1	0.0	66.7	21.0	66.7
19	Blade length: width > 4:1	lw_5	Ratio L/W: > 4:1	0.0	27.3	4.3	27.3
20	Shape of blade: obovate	sh_obov	Largest width in upper 2/5 of lamina	0.0	20.0	4.4	20.0
21	Shape of blade: elliptic	sh_elli	Largest width in middle 1/5 of lamina	43.5	96.9	81.0	53.4
22	Shape of blade: ovate	sh_ovat	Largest width in lower 2/5 of lamina	0.0	43.5	13.4	43.5

(lw_2), leaf L: W ratio > 4:1 (lw_5), ovate leaf shape (sh_ovat), leaf L: W ratio < 1:1 (lw_1) and obovate leaf shape (sh_obov) (Figs. 2, 3 and S1; Table 2). However, other leaf characters decreased with latitude, including leaf simple (le_simp), notophyll leaf size (ls_noto), mesophyll leaf size (ls_meso), leaf base acute (ba_acut), leaf L: W ratio = 2–4:1 (lw_3 and lw_4), elliptic leaf shape (sh_elli), leptophyll leaf size (ls_lept), leaf apex acute (ap_acut), leaf apex reflex (ap_refl) (Figs. 2, 3 and S1; Table 2) and untoothed leaf margins (untooth) (Fig. 2; Chen et al., 2014).

3.2. Correlation between leaf physiognomic characters and climate on single linear regressions (SLR)

The correlation matrix (Table 3) reveals that, except for ls_lept, lw_1 and sh_obov ($P > 0.01$), leaf physiognomic characters are significantly correlated with temperature-related climatic parameters ($P < 0.01$), such as MAT, Tsum, CMMT and WMMT, as well as with GSL, a parameter which also depends on temperature China. In general, the highest correlation with leaf physiognomy is CMMT, and the lowest correlation with leaf physiognomy is WMMT.

Precipitation-related parameters also have a significant correlation with leaf physiognomic characters ($P < 0.01$; Table 3), except for ls_lept, lw_1, ap_refl and sh_obov in humid regions in China ($P > 0.01$; Table 3). Among the eight precipitation parameters, GSP, MAP and P3WET show the highest correlations to specific leaf characters. Lw_2 recorded the strongest correlation with precipitation parameters, e.g., for GSP, $r = -0.707$, $P < 0.0001$. In general, the leaf physiognomic characters seem to be more affected by P3WET than by P3DRY.

Notably, the majority of leaf physiognomic characters, such as le_lobe, untooth, ls_micr, ls_noto, ba_acut, ba_refl, lw_2, lw_3 and sh_obov, not only have a significant correlation with temperature-related parameters, such as MAT, CMMT and GSL, they are also significantly correlated with precipitation-related parameters such as GSP, MAP and P3WET (Table 3).

3.3. Correlation between leaf physiognomic characters and climate parameters based on multiple linear regressions (MLR)

In order to compare our results with univariate analysis, the application of MLR based on thirteen different climatic parameters allows for a more detailed view on the relationship between leaf physiognomy and climate (Table 4). These transfer functions show strong correlations between leaf physiognomic characters and climatic parameters ($r^2 > 0.27$, $P < 10^{-51}$). The coefficients of determinations based on MLR transfer functions are commonly higher than the SLR transfer functions (Tables 3 and 4), e.g. concerning MAT, r^2 increases from 0.53 ($P < 0.0001$; Table 3) to 0.69 ($P < 10^{-181}$; Table 4); and for MAP, r^2 increase from 0.34 ($P < 0.0001$; Table 3) to 0.60 ($P < 10^{-144}$; Table 4). The highest correlation with leaf physiognomy was CMMT ($r^2 = 0.76$, $P < 10^{-224}$), and the lowest correlation with physiognomy was MMGSP ($r^2 = 0.28$, $P < 10^{-51}$). The factors ls_nano, lw_2, ba_acut, untooth and ls_micr represent some of the main factors in MLR. Our MLR transfer function based on the Chinese dataset for MAT was defined as (Table 4):

$$\mathrm{MAT} = 15.07 - 0.529 \times \mathrm{ls\_nano} - 0.121 \times \mathrm{lw\_2} + 0.104 \times \mathrm{untooth} + 0.482 \times \mathrm{ap\_refl} \quad (1)$$

with $r^2 = 0.69$, $F = 401.44$, SE = 2.51, $P = 2.2 \times 10^{-182}$.

In regard to MAP, the MLR transfer function was defined as (Table 4):

$$\mathrm{MAP} = 784.78 - 33.075 \times \mathrm{ls\_nano} - 15.683 \times \mathrm{lw\_5} + 14.776 \times \mathrm{ba\_acut} - 8.617 \times \mathrm{ls\_micr} \quad (2)$$

with $r^2 = 0.60$, $F = 277.82$, SE = 253.94, $P = 7.9 \times 10^{-145}$.

The patterns of variable predicted MAT using our Eq. (1) across humid regions in China is clearly related to latitude rather than actual MAT (Fig. 4a). The residual values (predicted MAT minus actual MAT values) plot (Fig. 4c) reveals a spatial pattern representing regions with systematic underestimations and overestimations. MAT is slightly overestimated (by 3.0–6.0 °C) in northern China, Tibet and Yunnan provinces, whereas larger overestimates (6.0–10.5 °C) occur in northeastern China, Qinghai-Tibet Plateau and Hengduan Mountains (colored red in Fig. 4c). In contrast, a slight underestimation of MAT (3.0–6.0 °C) can be observed in parts of Hainan province, whereas larger underestimations of MAT (6.0–6.9 °C) occur in Shanxi and Henan provinces in central China (Fig. 4c: green).

In contrast to MAT, the distribution pattern of predicted MAP using our Eq. (2) recorded a decrease along a gradient from the southeast to the northwest (Fig. 5b). The residual values (predicted MAP minus actual MAP values) plot (Fig. 5c) also identifies a spatial pattern representing regions with systematic underestimations and

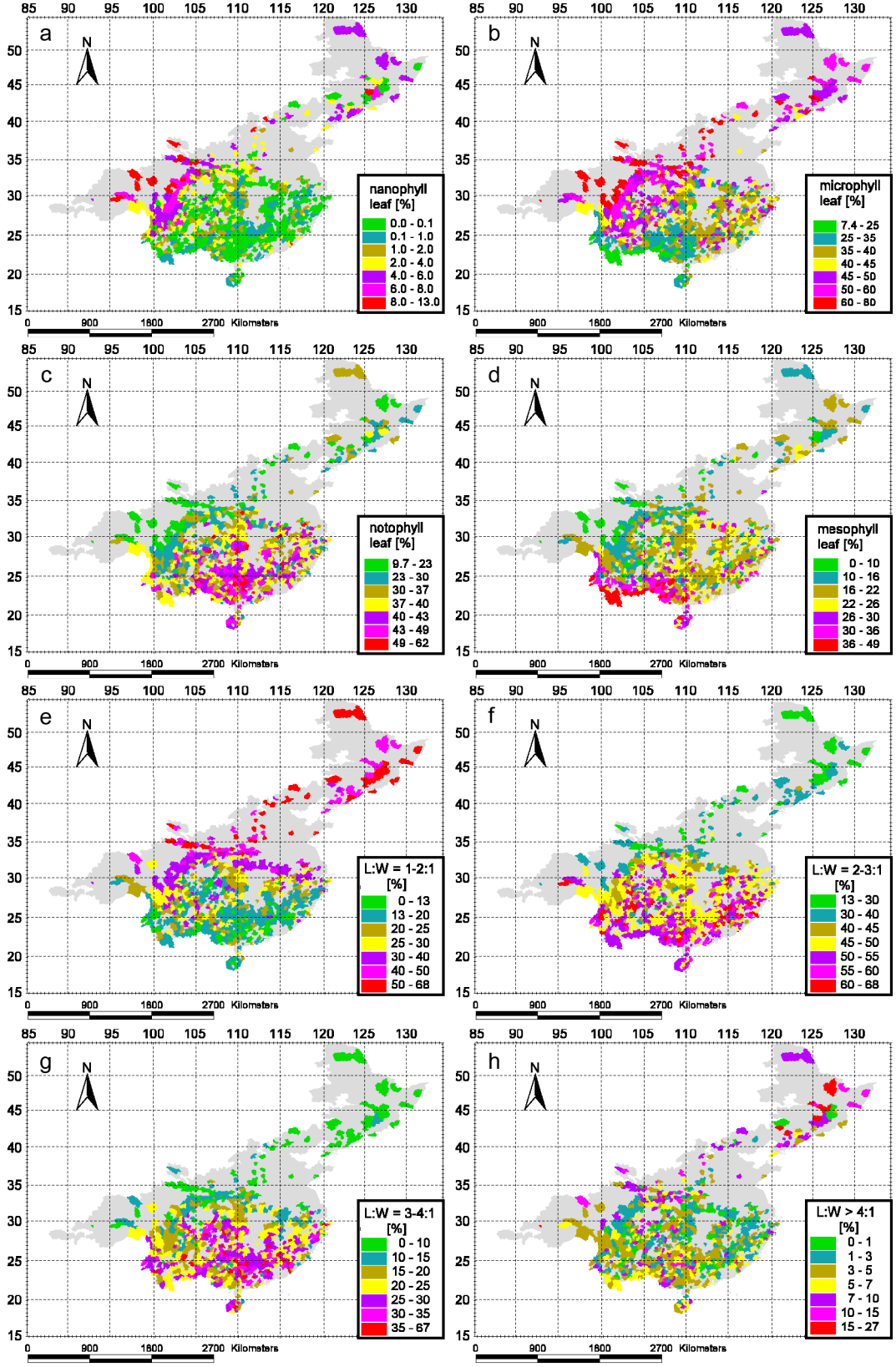

Fig. 2. Distribution patterns of the percentage of leaf physiognomic characters among Chinese native trees: a, color coded by nanophyll leaf size (ls_nano); b, color coded by microphyll leaf size (ls_micr); c, color coded by notophyll leaf size (ls_noto); d, color coded by mesophyll leaf size (ls_meso); e, color coded by leaf L: W ratio = 1–2:1 (lw_2); f, color coded by leaf L: W ratio = 2–3:1 (lw_3); g, color coded by leaf L: W ratio = 3–4:1 (lw_4); h, color coded by leaf L: W ratio > 4:1 (lw_5).

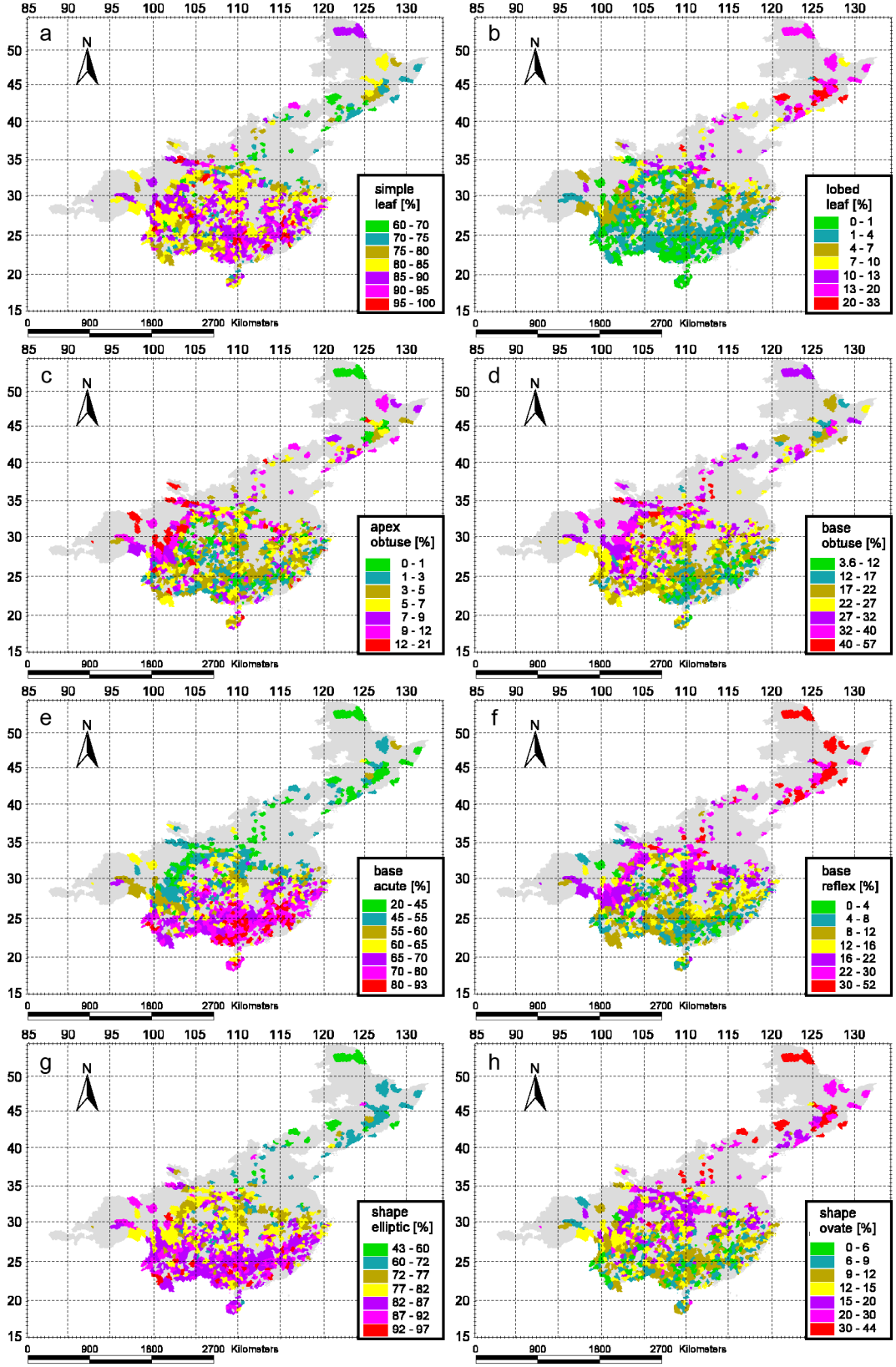

Fig. 3. Distribution patterns of the percentage of leaf physiognomic characters among Chinese native trees: a, color coded by leaf simple (le_simp); b, color coded by leaf lobe (le_lobe); c, color coded by leaf apex obtuse (ap_obtu); d, color coded by leaf base obtuse (ba_obtu); e, color coded by leaf base acute (ba_acut); f, color coded by leaf base reflex (ba_refl); g, color coded by elliptic leaf shape (sh_elli); h, color coded by ovate leaf shape (sh_ovat).

Table 2
Correlations between leaf physiognomic characters and geography. (*r*) correlation coefficients; for all correlations calibration grids, n = 732; leaf physiognomic characters abbreviations see Table 1.

Leaf character	Latitude		Longitude	
	r	*P*-values	*r*	*P*-values
le_simp	−0.362	< 0.0001	−0.103	0.005
le_lobe	0.754	< 0.0001	0.337	< 0.0001
untooth	−0.810	< 0.0001	−0.202	< 0.0001
ls_lept	−0.122	0.001	−0.110	0.003
ls_nano	0.386	< 0.0001	−0.237	< 0.0001
ls_micr	0.611	< 0.0001	0.018	0.635
ls_noto	−0.528	< 0.0001	0.051	0.169
ls_meso	−0.453	< 0.0001	−0.006	0.867
ap_obtu	0.236	< 0.0001	−0.105	0.005
ap_acut	−0.097	0.009	0.141	< 0.0001
ap_refl	−0.333	< 0.0001	−0.120	0.001
ba_obtu	0.449	< 0.0001	−0.182	< 0.0001
ba_acut	−0.714	< 0.0001	0.036	0.332
ba_refl	0.726	< 0.0001	0.245	< 0.0001
lw_1	0.367	< 0.0001	0.108	0.004
lw_2	0.802	< 0.0001	0.202	< 0.0001
lw_3	−0.676	< 0.0001	−0.167	< 0.0001
lw_4	−0.656	< 0.0001	−0.150	< 0.0001
lw_5	0.257	< 0.0001	0.003	0.940
sh_obov	0.300	< 0.0001	0.281	< 0.0001
sh_elli	−0.675	< 0.0001	0.305	< 0.0001
sh_ovat	0.657	< 0.0001	0.186	< 0.0001

overestimations. MAP is slightly overestimated (250–500 mm) in southwest China, whereas larger overestimates (500–623 mm) mainly occur in the Yun-Gui Plateau in southwest China (Fig. 5c: red). In contrast, a slight underestimation of MAP (250–500 mm) can be observed in southeast China, whereas larger underestimates (500–927 mm) mainly occur in Hainan, Guangdong and Guangxi provinces in southern China (Fig. 5c: green).

4. Discussion

4.1. Distribution patterns of leaf physiognomy and climate

Results from our study indicate that clear latitudinal spatial distribution patterns exist for all leaf characters (Figs. 2, 3 and S1; Table 2). These patterns are mainly controlled by a combination of temperature (predominantly CMMT) and precipitation (predominantly GSP) in humid regions in China (Table 3). Findings from this study demonstrate that a significant relationship between leaf physiognomic characters was determined by species and climate across humid regions in China. Leaf characters do not only correlate with temperature-related parameters, such as MAT, CMMT and GSL, but also with precipitation-related parameters, such as GSP, MAP and P3WET. In particular, leaf physiognomic characters seem to be more affected by CMMT than other temperature-related parameters, and more affected by GSP than other precipitation-related parameters (Table 3).

This finding is consistent with previous observations reporting that leaf physiognomic characters might be affected by both temperature and precipitation (Wolfe, 1993; Wiemann et al., 1998; Wilf et al., 1998; Jacobs, 1999; Peppe et al., 2011; Li et al., 2016; Wright et al., 2017). For example, Peppe et al. (2011), using 92 global sites, recorded leaf physiognomy may be affected by MAT and MAP. Recently, Wright et al. (2017) observed that both temperature (mean temperature during the warmest month) and moisture (MAP) showed strong interactive effects in leaf size variation using 682 global nonagricultural sites. The influence of interacted climatic variables on leaf physiognomy in humid regions in China may be due to several reasons. Firstly, previous studies have shown that several simultaneously occurring climatic variables can synergistically interact (O'Brien, 2006; Stephenson, 1990). In our study areas, temperature-related parameters recorded a significant correlation with precipitation-related parameters ($r > +0.240$, $P < 0.001$; Table 5) which may account for overall leaf physiognomy being controlled by both temperature and precipitation. Secondly, previous studies found that water–energy dynamics mainly contributed to influence woody plant life and its spatial distribution globally

Table 3
Correlation matrix of leaf physiognomic characters and climatic parameters. (*r*) correlation coefficients; the statistical significance is indicated as: $^{***}P < 0.0001$, $^{**}P < 0.001$, $^{*}P < 0.01$, ns $P > 0.01$; for all correlations calibration grids, n = 732; leaf physiognomic characters for abbreviations see Table 1; climate abbreviations: MAT: Mean Annual Temperature (°C), Tsum: Annual Temperature Sum (°C), WMMT: Warmest Month Mean Temperature (°C), CMMT: Coldest Month Mean Temperature (°C), GSL: Length of the Growing Season (month), MAP: Mean Annual Precipitation (mm), GSP: Growing Season Precipitation (mm), MMGSP: Mean Monthly Growing Season Precipitation (mm), Pmax: the Wettest Month Precipitation (mm), Pmin: the Driest Month Precipitation (mm), P3WET: Precipitation during Three Wettest Consecutive Months (mm), P3DRY: Precipitation during Three Driest Consecutive Months (mm), RH: Relative Humidity (%); [a] the *r* between untooth and MAT, WMMT and CMMT are from Chen et al. (2014).

r	MAT	Tsum	WMMT	CMMT	GSL	MAP	GSP	MMGSP	Pmax	Pmin	P3WET	P3DAR	RH
le_simp	0.264***	0.267***	0.135***	0.295***	0.233***	0.364***	0.355***	0.287***	0.228***	0.341***	0.283***	0.340***	0.218***
le_lobe	−0.654***	−0.656***	−0.237***	−0.745***	−0.628***	−0.506***	−0.557***	−0.282***	−0.391***	−0.305***	−0.466***	−0.307***	−0.382***
[a]untooth	0.725***	0.728***	0.313***	0.771***	0.758***	0.586***	0.655***	0.302***	0.507***	0.334***	0.559***	0.351***	0.439***
ls_lept	0.071ns	0.071ns	−0.085ns	0.125**	0.122**	−0.024ns	0.013ns	−0.071ns	0.028ns	−0.100*	0.021ns	−0.106*	−0.132ns
ls_nano	−0.524***	−0.525***	−0.579***	−0.407***	−0.466***	−0.351***	−0.518***	−0.371***	−0.383***	−0.524***	−0.412***	−0.529***	−0.567***
ls_micr	−0.639***	−0.640***	−0.435***	−0.606***	−0.651***	−0.589***	−0.615***	−0.370***	−0.494***	−0.406***	−0.531***	−0.426***	−0.519***
ls_noto	0.561***	0.564***	0.462***	0.508***	0.521***	0.570***	0.567***	0.406***	0.426***	0.483***	0.471***	0.502***	0.511***
ls_meso	0.490***	0.489***	0.315***	0.463***	0.536***	0.409***	0.447***	0.219***	0.381***	0.236***	0.395***	0.248***	0.373***
ap_obut	−0.340***	−0.340***	−0.369***	−0.265***	−0.321***	−0.343***	−0.352***	−0.251***	−0.257***	−0.281***	−0.290***	−0.271***	−0.375***
ap_actu	0.189***	0.189***	0.287***	0.114*	0.164***	0.257***	0.248***	0.229***	0.185***	0.230***	0.209***	0.223***	0.355***
ap_refl	0.337***	0.339***	0.150***	0.355***	0.364***	0.151***	0.202***	−0.004ns	0.134***	0.060ns	0.151***	0.053ns	−0.068ns
ba_obtu	−0.457***	−0.457***	−0.400***	−0.384***	−0.464***	−0.570***	−0.563***	−0.432***	−0.446***	−0.539***	−0.488***	−0.555***	−0.494***
ba_acut	0.659***	0.662***	0.403***	0.651***	0.660***	0.680***	0.705***	0.453***	0.534***	0.554***	0.608***	0.565***	0.578***
ba_refl	−0.626***	−0.631***	−0.259***	−0.687***	−0.618***	−0.544***	−0.594***	−0.310***	−0.430***	−0.368***	−0.507***	−0.366***	−0.465***
lw_1	−0.293***	−0.298***	−0.069ns	−0.324***	−0.351***	−0.259***	−0.309***	−0.114*	−0.250***	−0.111*	−0.287***	−0.108*	−0.178**
lw_2	−0.728***	−0.727***	−0.371***	−0.767***	−0.702***	−0.669***	−0.707***	−0.449***	−0.534***	−0.469***	−0.610***	−0.476***	−0.564***
lw_3	0.637***	0.637***	0.324***	0.674***	0.608***	0.539***	0.572***	0.334***	0.445***	0.352***	0.505***	0.358***	0.399***
lw_4	0.574***	0.575***	0.309***	0.601***	0.546***	0.571***	0.590***	0.401***	0.431***	0.452***	0.495***	0.454***	0.542***
lw_5	−0.277***	−0.278***	−0.232***	−0.282***	−0.187***	−0.244***	−0.207***	−0.167***	−0.141***	−0.282***	−0.159***	−0.281***	−0.235***
sh_obov	−0.193***	−0.197***	0.077ns	−0.286***	−0.234***	−0.059ns	−0.117*	0.071ns	−0.011ns	0.055ns	−0.071ns	0.073ns	0.107ns
sh_elli	0.517***	0.520***	0.123**	0.610***	0.522***	0.447***	0.484***	0.244***	0.345***	0.293***	0.423***	0.289***	0.250***
sh_ovat	−0.542***	−0.543***	−0.224***	−0.594***	−0.522***	−0.530***	−0.543***	−0.352***	−0.431***	−0.403***	−0.488***	−0.408***	0.381***

Table 4
Multiple linear regression transfer functions of different climatic parameters. (b_0) constant; (b_1, b_2, b_3, b_4) coefficient; (x_1, x_2, x_3, x_4) leaf physiognomic character, for abbreviations see Table 1; (r^2) coefficients of determination; (*F*) *F*-value; (SE) standard error; (*P*) *P*-values; for all MLR transfer functions calibration grids, n = 732; climate abbreviations and units see Table 3.

	Y	b_0	b_1	x_1 (%)	b_2	x_2 (%)	b_3	x_3 (%)	b_4	x_4 (%)	r^2	*F*	SE	*P*
1	MAT	15.07	−0.529	ls_nano	−0.121	lw_2	0.104	untooth	0.482	ap_refl	0.69	401.44	2.51	10^{-182}
2	Tsum	179.33	−6.312	ls_nano	−1.420	lw_2	1.267	untooth	5.750	ap_refl	0.69	407.21	29.66	10^{-184}
3	WMMT	25.31	−0.696	ls_nano	0.070	ls_noto	−0.062	ba_obtu	0.316	ap_refl	0.40	124.49	2.74	10^{-81}
4	CMMT	4.28	−0.403	le_lobe	−0.145	lw_2	0.186	untooth	−0.373	lw_5	0.76	585.33	3.39	10^{-225}
5	GSL	7.26	0.076	ls_meso	−0.035	lw_2	0.046	untooth	−0.063	ba_refl	0.67	378.64	1.21	10^{-176}
6	MAP	784.78	−33.075	ls_nano	−15.683	lw_5	14.776	ba_acut	−8.617	ls_micr	0.60	277.82	253.94	10^{-145}
7	GSP	1098.54	−32.410	ls_nano	−6.887	lw_2	10.084	ba_acut	−8.794	ls_micr	0.64	319.47	242.73	10^{-158}
8	MMGSP	49.19	−1.783	ls_nano	0.611	ls_noto	0.804	ba_acut	1.493	sh_obov	0.28	73.39	25.58	10^{-52}
9	Pmax	234.04	−3.450	ls_nano	−0.786	lw_2	1.352	ba_acut	−1.469	ls_micr	0.37	109.1	55.45	10^{-73}
10	Pmin	20.83	−1.933	ls_nano	−0.970	lw_5	0.314	ba_acut	−0.432	ba_obtu	0.46	155.42	11.82	10^{-96}
11	P3WET	602.02	−8.985	ls_nano	−2.931	lw_2	4.195	ba_acut	−3.847	ls_micr	0.46	157.71	138.73	10^{-96}
12	P3DRY	82.51	−6.906	ls_nano	−3.467	lw_5	1.100	ba_acut	−1.713	ba_obtu	0.47	163.8	41.95	10^{-100}
13	RH	48.41	−0.739	ls_nano	−0.140	ls_micr	0.156	ba_acut	0.271	ap_acut	0.54	102.85	3.81	10^{-57}

(Woodward et al., 2004; O'Brien, 2006). Ge and Xie (2017) also found that CMMT and MAP interacted to significantly control the geographical distribution of broad-leaved tree species in subtropical China. These findings indicate that the interaction of climatic variables not only affects the distribution of plants, they also affect the distribution of leaf physiognomy in China. Thirdly, and perhaps most importantly, leaf physiognomy is significantly influenced by the Asian monsoon climate in China.

4.2. The impact of the Asian Monsoon regime on leaf physiognomy

Climate affected by the Asian Monsoon has significant characteristics, especially for precipitation patterns, such as abundant rainfall during the summer and drought periods during the winter (Lau and Chan, 1983). It is proposed that P3WET and P3DRY could represent leaf physiognomy response to the monsoon climate (Jacques et al., 2011; Xing et al., 2012; Khan et al., 2014). In this study, large differences between P3WET and P3DRY for most grids (Supplementary Data 2) were recorded, indicating that these humid areas were affected by the Asian Monsoon (Wang et al., 2006).

Under the Asian monsoon climate, results in our study indicate that leaf physiognomic characters correlate more closely with P3WET than P3DRY. This result is consistent with previous results exposed to Asian monsoon climates characterized by marked wet and dry seasons. For instance, Jacques et al. (2011) found that Chinese sites were grouped together and separated away from others in physiognomic space using CCA; P3WET and P3DRY vectors in the Chinese sites indicated high precipitation values. Su et al. (2013) also observed that untoothed leaf margin showed a weak correlation with P3DRY, whereas they had a high correlation with P3WET. In southern China, where experiences the monsoon climate, leaves of evergreen trees have to adapt to both dry and wet climatic conditions, while leaves of deciduous leaves only have to adapt to wet climatic conditions (Kennedy et al., 2014). Leaves of woody plants have to adapt to extremes due to seasonal climatic variation, therefore resulting in unique monsoon 'fingerprints' encoded in leaf physiognomy (Spicer, 2017). It is not surprising that leaf physiognomic spectra are distinctive in Asian monsoon climates (Jacques et al., 2011; Spicer et al., 2016); in our study we observed leaf physiognomic characters to be more affected by P3WET than by P3DRY. Overall, results from our study demonstrate that leaf physiognomic characters have the highest correlation with CMMT and GSP, and leaf physiognomic characters are more affected by P3WET than by P3DRY. This indicates that the distribution of leaf physiognomy in China is controlled by both cold winters (plant survival) and abundant water sources in the summer (plant growth). This finding provides a simple explanation that overall leaf physiognomic characters are significantly controlled by both temperature and precipitation in humid regions in China.

4.3. Correlation between leaf physiognomic characters and climatic parameters using multiple linear regressions (MLR)

Results from our study show that relationships between climate and leaf physiognomy using MLR are higher than those obtained using SLR. This result is consistent with previous results based on multivariate analysis of leaf physiognomy, where leaf physiognomy simultaneously integrates more characters that have a functional and/or physiological connection to climate (Wolfe, 1993; Royer et al., 2005, 2008; Traiser et al., 2005; Peppe et al., 2011; Kennedy et al., 2014; Yang et al., 2015).

MLR transfer functions (Table 4) indicated that the highest correlation with leaf physiognomy was CMMT ($r^2 = 0.76$, $P = 10^{-225}$), a result that differs from previous studies (Wing and Greenwood, 1993; Gregory, 1996; Traiser et al., 2005; Yang et al., 2015). Although the MLR transfer function of CMMT has the highest coefficient of determination, the standard error (SE) of CMMT estimation was very high, with 3.39 °C (SE = 2.51, MAT). This result may be due to CMMT including a large range of climate parameters with a wide variation, thus having a greater standard deviation (Yang et al., 2015). Moreover, vegetation in northern China and vegetation at high elevations are predominantly deciduous species. Because deciduous trees have no leaf during the winter, they would experience low selection pressures that influence leaf physiognomy at that season. Consequently, CMMT is not only indirectly correlated with leaf physiognomy (Spicer et al., 2004). Therefore, reconstruction of CMMT using leaf physiognomy from MLR transfer functions does not provide better results than using MAT.

Moreover, in comparison to previous studies using MLR transfer functions of MAT (Wing and Greenwood, 1993; Gregory and McIntosh, 1996; Wiemann et al., 1998; Traiser et al., 2005; Lielke et al., 2012), results from our study indicate a weaker coefficient of determination for this parameter (Table 6). Firstly, our study region experiences a strong Asian monsoon climate characterized by marked variations in seasonal precipitation. Previous studies observed that seasonality of rainfall could influence leaf physiognomy-climate correlations (Wolfe, 1993; Wing and Greenwood, 1993; Jacques et al., 2011; Su et al., 2013; Jacques et al., 2014; Yang et al., 2015; Spicer et al., 2016). Therefore, the East Asian monsoon climate may affect the relationships between integrated leaf characters and temperature. Secondly, our study includes a large-scale dataset which covers a more extensive area and a wider range of climates. It seems that the wider range of climate and spatial range for each grid, the weaker the coefficient of determination (Peppe et al., 2011; Chen et al., 2014; Kennedy et al., 2014). Results in this study were obtained using county-scale climate data (area size and climate data notably varied), thus it might add 'noise' to the leaf physiognomy-climate relationships (Chen et al., 2014).

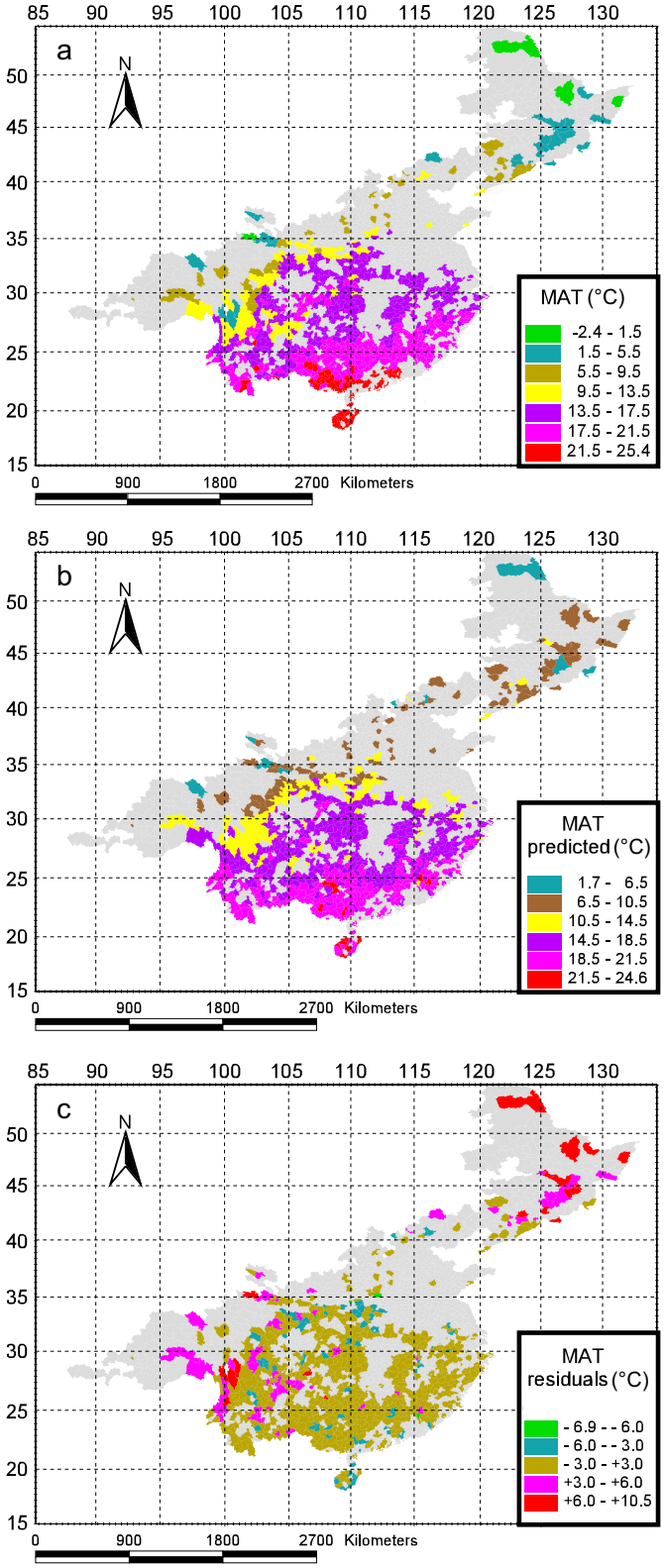

Fig. 4. Mean Annual Temperature (MAT) distribution pattern. (a) Actual MAT (Chen et al., 2014); (b) predicted MAT from the transfer function; (c) residuals of predicted MAT minus actual MAT values. (For interpretation of the references to color in this figure, the reader is referred to the web version of this article.)

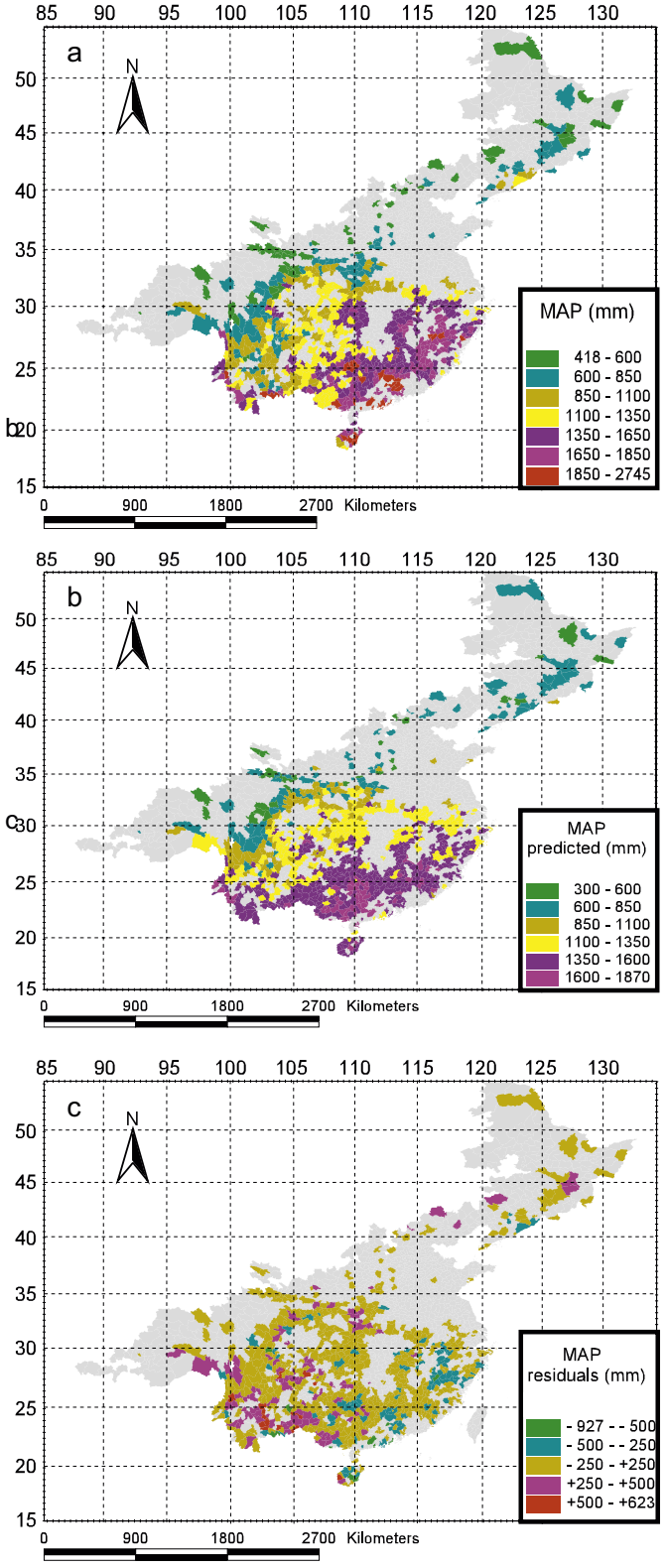

Fig. 5. Mean Annual Precipitation (MAP) distribution pattern. (a) Actual MAP (Chen et al., 2014); (b) predicted MAP from the transfer function; (c) residuals of predicted MAP minus actual MAP values. (For interpretation of the references to color in this figure, the reader is referred to the web version of this article.)

Table 5
Pearson correlations among climate variables. (*r*) correlation coefficients; the statistical significance for all: $P < 0.001$; for all Pearson correlations calibration grids, n = 732; climate abbreviations and units see Table 3.

r	MAT	Tsum	WMMT	CMMT	GSL	MAP	GSP	MMGSP	Pmax	Pmin	P3WET	P3DAR	RH
MAT	1	0.999	0.727	0.945	0.914	0.702	0.771	0.346	0.571	0.494	0.623	0.505	0.499
Tsum	0.999	1	0.725	0.944	0.915	0.703	0.771	0.341	0.571	0.495	0.624	0.506	0.450
WMMT	0.727	0.725	1	0.476	0.542	0.578	0.561	0.369	0.374	0.560	0.387	0.660	0.376
CMMT	0.945	0.944	0.476	1	0.895	0.632	0.718	0.284	0.534	0.355	0.598	0.362	0.382
GSL	0.914	0.915	0.542	0.895	1	0.641	0.759	0.243	0.583	0.357	0.639	0.361	0.354
MAP	0.702	0.703	0.578	0.632	0.641	1	0.975	0.853	0.868	0.769	0.918	0.782	0.720
GSP	0.771	0.771	0.561	0.718	0.759	0.975	1	0.776	0.887	0.660	0.938	0.671	0.702
MMGSP	0.346	0.341	0.369	0.284	0.243	0.853	0.776	1	0.765	0.675	0.785	0.686	0.643
Pmax	0.571	0.571	0.374	0.534	0.583	0.868	0.887	0.765	1	0.482	0.968	0.487	0.555
Pmin	0.494	0.495	0.560	0.355	0.357	0.769	0.660	0.675	0.482	1	0.534	0.984	0.621
P3WET	0.623	0.624	0.387	0.598	0.639	0.918	0.938	0.785	0.968	0.534	1	0.543	0.601
P3DAR	0.505	0.506	0.660	0.362	0.361	0.782	0.671	0.686	0.487	0.984	0.543	1	6.609
RH	0.499	0.450	0.376	0.382	0.354	0.720	0.702	0.643	0.555	0.621	0.601	6.609	1

4.4. Estimating climate from leaf physiognomy based on MLR transfer functions

4.4.1. Estimating MAT from the MLR transfer function

The distribution pattern of predicted MAT values in humid regions in China based on the MLR transfer function (Fig. 4b) shows a clear latitudinal pattern compared to results using actual MAT values (Fig. 4a). Results from the residual MAT plot also indicate that most areas are within ± 2.51 °C (Fig. 4c). Therefore, our result demonstrates that the MLR transfer function of MAT is suitable for predicting realistic values based on leaf physiognomy-climate correlations in China. In particular, compared with the residual value from the SLR transfer function with similar calibration datasets (Fig. 6c; Chen et al., 2014), our residual values from the MLR transfer function show that the highest overestimate values of MAT declines from 11.3 °C to 10.5 °C, and the lowest underestimate values of MAT increase from −9.7 °C to −6.9 °C. Our multivariate MAT model is therefore more accurate and precise than a similarly calibrated leaf-margin analysis equation.

However, limits in the accuracy of temperature estimated from the multivariate MAT model using synthetic chorologic flora are highlighted in our results, therefore reconstructed palaeoclimate results have substantially overestimated or underestimated MATs in some regions in China. The spatial distribution of the residual plot of MAT (Fig. 4c) reveals that large MAT overestimates (6.0–10.5 °C) mainly occurs in the northeast of China, the Qinghai-Tibetan Plateau and Hengduan Mountains. These areas have extreme cold temperatures and complex topography. For areas with extreme cold temperatures in northeastern China (MAT < 5.2 °C), it may not be suitable to estimate palaeoclimate based on leaf physiognomy effects using leaf habit; deciduous habits may have a greater effect than evergreen habits (Chen et al., 2014). Difficulties in obtaining good predictions for cold regions have also been observed for climatic estimates based on leaf physiognomy (Spicer et al., 2004), for example Yang et al. (2015) showed that samples from extremely cold climates in Asiatic Russia (Siberia) were plotted apart from other regions. In addition, for the Qinghai-Tibetan Plateau and Hengduan Mountains, alpine nest sites (WMMT < 13.2 °C and CMMT less than −3.1 °C) are known to lower the accuracy and precision of temperature reconstructions based on leaf physiognomy (Wolfe, 1993). This result differs from previous studies based on the CLAMP dataset in China where the effect of the 'alpine nest' has not been previously tested (Jacques et al., 2011). Results in our study also differ from previous studies due to the large study area, which includes a wide variation of climate and leaf physiognomy in our dataset. By contrast, larger underestimations of MAT (6.0–6.9 °C) (Fig. 4c) occurred in Shanxi (Tanghang Mountains) and Henan provinces (Dabie Mountains), areas which have complex terrain. The very broad ranges of altitude at country sizes can produce locally more extreme climates in complex topography regions. It could affect the estimated temperature in those areas. Therefore, together with extremely cold temperatures, alpine climatic regions and areas with complex topography can increase estimation biases of the derived equations.

4.4.2. Estimating MAP from the MLR transfer function

In contrast to MAT, the distribution pattern of predicted MAP from the MLR transfer function shows a clear pattern in humid regions in China (Fig. 5b). Results indicated that there was a reduction from the southeast coast to the northwest interior (Fig. 5b), and the most regional of residual MAP are in standard deviation of the transfer function (SE) ± within 253.94 mm range (Fig. 5c). In addition, our results showed that the multi-linear transfer function of MAP from leaf physiognomy had a high correlation coefficient of determination ($r^2 = 0.60$, $P = 10^{-145}$). This result differed from those of Traiser et al. (2005) who used the same method based on the European dataset (MLR, $r^2 = 0.26$, $P < 10^{-5}$; SE = 143.4 mm), and from those of Peppe et al. (2011) who examined digital leaf physiognomy using the global dataset (MLR, $r^2 = 0.27$, $P = 10^{-6}$; SE = 0.60 ($\log_e$, cm)). Thus, our study demonstrates that reconstructing precipitation based on the MLR transfer function of MAP with leaf physiognomy is a useful method for areas experiencing an Asian monsoon climate.

Similarly, the MAP residual plot (Fig. 5c) also highlighted a distribution pattern representing regions with systematic underestimation and overestimation of MAPs. For example, significant MAP overestimates (500–623 mm) occurred in the Yun-Gui Plateau in southwest China, with the transitional area (TA) for the East Asian Monsoon (EAM) and the South Asian Monsoon (SAM) (Wang and Ho, 2002). In contrast, extreme underestimation of MAP (500–927 mm) was observed in Hainan, Guangdong and Guangxi provinces in southern China, with TA or close to TA (Wang and Ho, 2002). MAP predicted values were largely overestimated or underestimated mainly in TA, which experiences the influence of both Asian monsoon systems. There are complex seasonal rainfall variations in these areas (Wang and Ho, 2002), thus they could potentially affect the accuracy on estimating MAP. Therefore, it is not surprising that predicted MAPs have a low accuracy in this area. Therefore, in the transitional areas for EAM and SMA, the MLR transfer function of MAP also has limitations for reconstructing precipitation in China.

5. Conclusions

Analysis of the relationships between modern leaf physiognomic characters and climatic parameters based on a large-scale dataset in humid regions in China were investigated. Our results show the existence of a significant correlation between leaf physiognomic characters and climate parameters, in which the distribution patterns of leaf characters are correlated with both temperature-related parameters (most notably CMMT) and precipitation-related parameters (most

Table 6
Multiple linear regression transfer functions of Mean Annual Temperature (MAT) based on different calibration data sets from different regions across the world. (b_0) constant; (b_1, b_2, b_3 …) coefficient; (x_1, x_2, x_3 …) leaf physiognomic character, abbreviations see Table 1; (n) number of samples; (r^2) coefficient of determination; (SE) standard error; (*) this function not include the regular teeth and acute teeth.

	Y	b_0	b_1	x_1 (%)	b_2	x_2 (%)	b_3	x_3 (%)	b_4	x_4 (%)	b_5	x_5 (%)	b_6	x_6 (%)	n	r^2	SE	Author
1	MAT	2.54	17.372	Untooth	2.896	ap_refl	−8.592	lw_1	–	–	–	–	–	–	74	0.86	2.0	Wing and Greenwood, 1993; Traiser et al., 2005
2	MAT	1.77	16.656	Untooth	4.879	ap_refl	−5.594	lw_1	5.137	ba_acut	−9.200	ls_nano	–	–	106	0.92	1.5	Gregory, 1996; Traiser et al., 2005
3	MAT	−11.26	23.258	Untooth	7.022	ba_acut	−16.099	lw_1	10.282	le_lobe	−12.210	ls_nano	11.484	lw_2	106	0.89	2.3	Gregory and McIntosh, 1996; Traiser et al., 2005
4	MAT	9.87	0.207	Untooth	−0.058	ba_acut	−2.202	lw_1	–	–	–	–	–	–	144	0.90	2.8	Wiemann et al., 1998
5	MAT	2.60	0.142	Untooth	0.210	ba_acut	0.140	lw_3	−0.249	sh_obov	–	–	–	–	1835	0.89	0.9	Traiser et al., 2005
6	MAT	12.85	0.157	Untooth	0.082	ap_refl	−0.219	lw_1	−0.045	ba_obtu	0.161	ls_nano	–	–	173	0.88	2.4	* Lielke et al., 2012
7	MAT	15.58	0.104	Untooth	0.482	ap_refl	−0.121	lw_2	−0.529	ls_nano	–	–	–	–	732	0.69	2.5	This study

notably GSP). In addition, seasonality rainfall variables affected by the Asian Monsoon might influence leaf physiognomic characters, which correlate with P3WET more than P3DRY. Our study demonstrates that multivariate methods are better reflected on leaf physiognomy-climate correlations rather than univariate methods. Our findings illustrate that the MLR transfer function using leaf physiognomic parameters based on a large-scale dataset represents a promising approach for predicting palaeoclimate in China. In future, MLR transfer functions of MAT may be improved by incorporating regional constraints (i.e., extremely cold temperatures, alpine environments and complex topography), and MLR transfer functions of MAP may also be significantly enhanced.

Supplementary data to this article can be found online at https://doi.org/10.1016/j.palaeo.2019.04.022.

Acknowledgments

We especially thank Dr. Falcon-Lang and anonymous reviewer for helpful comments and advice. This work was supported by NSFC-Yunnan Joint Fund to support key projects (No. U1502231), the Strategic Priority Research Program of Chinese Academy of Sciences (No. XDA20050204 and XDA19050301), Key Research Program of Frontier Sciences, CAS (QYZDB-SSW-SMC016), and Youth Innovation Promotion Association of the Chinese Academy of Sciences (2017439).

References

Adams, J.M., Green, W.A., Zhang, Y., 2008. Leaf margins and temperature in the North American flora: Recalibrating the paleoclimatic thermometer. Glob. Planet. Chang. 60, 523–534.

Ai, K., Shi, G.L., Zhang, K.X., Ji, J.L., Song, B.W., Shen, T.Y., Guo, S.X., 2019. The uppermost Oligocene Kailas flora from southern Tibetan plateau and its implications for the uplift history of the southern Lhasa terrane. Palaeogeogr. Palaeoclimatol. Palaeoecol. 515, 143–151. https://doi.org/10.1016/j.palaeo.2018.04.017.

Bailey, I.W., Sinnott, E.W., 1915. A botanical index of Cretaceous and Tertiary climates. Science 29, 384–395.

Bailey, I.W., Sinnott, E.W., 1916. The climatic distribution of certain types of angiosperm leaves. Am. J. Bot. 3, 24–39.

Bush, R.T., Wallace, J., Currano, E.D., Jacobs, B.F., Mcinerney, F.A., Dunn, R.E., Tabor, N.J., 2017. Cell anatomy and leaf $\delta^{13}C$ as proxies for shading and canopy structure in a Miocene forest from Ethiopia. Palaeogeogr. Palaeoclimatol. Palaeoecol. 485, 593–604.

Chen, W.Y., Su, T., Adams, J.M., Jacques, F.M.B., Ferguson, D.K., Zhou, Z.K., 2014. Large-scale dataset from China gives new insights into leaf margin-temperature relationships. Palaeogeogr. Palaeoclimatol. Palaeoecol. 402, 73–80.

Chen, Y.S., Deng, T., Zhou, Z., Sun, H., 2018. Is the East Asian flora ancient or not? National Science Review 0, 1–13.

Dilcher, D.L., 1973. A paleoclimatic interpretation of the Eocene floras of southeastern North America. In: Graham, A. (Ed.), Vegetation and Vegetational History of Northern Latin America. Elsevier, Amsterdam, the Netherlands, pp. 39–59.

Ellis, B., Daly, D., Hickey, L.J., Johnson, K.R., Mitchell, J., Wilf, P., Wing, S.L., 2009. Manual of Leaf Architecture. Cornell University Press, pp. 1–188.

Forest, C.E., Wolfe, J.A., Molnar, P., Emmanuel, K.A., 1999. Paleoaltimetry incorporating atmospheric physics and botanical estimates of paleoclimate. Geol. Soc. Am. Bull. 111, 497–511.

Ge, J., Xie, Z., 2017. Geographical and climatic gradients of evergreen versus deciduous broad-leaved tree species in subtropical China: implications for the definition of the mixed forest. Ecology and Evolution 7 (11), 3636–3644.

Givnish, T.J., 1984. Leaf and canopy adaptations in tropical forests. In: Medina, E., Mooney, H.A., Vasquez-Yanes, C. (Eds.), Physiological Ecology of Plants of the Wet Tropics. Dr. W. Junk Publishers, The Hague, the Netherlands, pp. 51–84.

Godefroit, P., Golvneva, L.B., Shchepetov, S., Garcia, G., Alekseev, P., 2009. The last polar dinosaurs: high diversity of latest Cretaceous Arctic dinosaurs in Russia. Naturwissenschaften 96, 495–501.

Greenwood, D.R., Wilf, P., Wing, S.L., Christophel, D.C., 2004. Paleotemperature estimation using leaf-margin analysis: is Australia different? Palaios 19, 129–142.

Greenwood, D.R., Basinger, J.F., Smith, R.Y., 2010. How wet was the Arctic Eocene rain forest? Estimates of precipitation from Paleogene Arctic macrofloras. Geology 38 (1), 15–18.

Gregory, K.M., 1994. Palaeoclimate and palaeoelevation of the 35 Ma Florissant flora, Front Range, Colorado. Palaeoclimates 1, 23–57.

Gregory, K.M., 1996. Are paleoclimate estimates biased by foliar physiognomic responses to increased atmospheric CO_2? Palaeogeogr. Palaeoclimatol. Palaeoecol. 124, 39–51.

Gregory, K.M., McIntosh, W.C., 1996. Paleoclimate and paleoelevation of the Oligocene Pitch-Pinnacle flora, Sawatch Range, Colorado. Geol. Soc. Am. Bull. 108, 546–561.

Gregory-Wodzicki, K.M., 2000. Relationship between leaf morphology and climate, Bolivia: implications for estimating paleoclimate from fossil floras. Paleobiology 26, 668–688.

Herman, A.B., Spicer, R.A., 1996. Palaeobotanical evidence for a warm Cretaceous Arctic

Ocean. Nature 380, 330–333.
Herman, A.B., Spicer, R.A., Aleksandrova, G.N., Yang, J., Kodrul, T.M., Maslova, N.P., Spicer, T.E.V., Chen, G., Jin, J.H., 2017. Eocene-early Oligocene climate and vegetation change in southern China: evidence from the Maoming Basin. Palaeogeogr. Palaeoclimatol. Palaeoecol. 479, 126–137.
Jacobs, B.F., 1999. Estimation of rainfall variables from leaf characters in tropical Africa. Palaeogeogr. Palaeoclimatol. Palaeoecol. 145, 231–250.
Jacobs, B.F., 2002. Estimation of low-latitude paleoclimates using fossil angiosperm leaves: examples from the Miocene Tugen Hills, Kenya. Paleobiology 28, 399–421.
Jacques, F.M.B., Su, T., Spicer, R.A., Xing, Y.W., Huang, Y.J., Wang, W.M., Zhou, Z.K., 2011. Leaf physiognomy and climate: are monsoon systems different? Glob. Planet. Chang. 76, 56–62.
Jacques, F.M.B., Shi, G.L., Li, H.M., Wang, W.M., 2014. An early-middle Eocene Antarctic summer monsoon: evidence of 'fossil climates'. Gondwana Res. 25 (4), 1422–1428.
Jordan, G.J., 2011. A critical framework for the assessment of biological palaeoproxies: predicting past climate and levels of atmospheric CO_2 from fossil leaves. New Phytol. 192 (1), 29–44.
Kennedy, E.M., Spicer, R.A., Rees, P.M., 2002. Quantitative paleoclimate estimates from Late Cretaceous and Paleocene leaf floras in the northwest of the South Island, New Zealand. Palaeogeogr. Palaeoclimatol. Palaeoecol. 184, 321–345.
Kennedy, E.M., Nan, C.A., Reichgelt, T., Spicer, R.A., Spicer, T.E.V., Stranks, L., Yang, J., 2014. Deriving temperature estimates from southern hemisphere leaves. Palaeogeogr. Palaeoclimatol. Palaeoecol. 412, 80–90.
Khan, M.A., Spicer, R.A., Bera, S., Ghosh, R., Yang, J., Spicer, T.E.V., Guo, S.X., Su, T., Jacques, F.M.B., Grote, P.J., 2014. Miocene to Pleistocene floras and climate of the Eastern Himalayan Siwaliks, and new palaeoelevation estimates for the Namling-Oiyug Basin, Tibet. Glob. Planet. Chang. 113, 1–10.
Kovach, W.L., Spicer, R.A., 1996. Canonical Correspondence Analysis of Leaf Physiognomy: a contribution to the development of a new palaeoclimatological Tool. Palaeoclimates 2, 125–138.
Kowalski, E.A., 2002. Mean annual temperature estimation based on leaf morphology: a test from tropical South America. Palaeogeogr. Palaeoclimatol. Palaeoecol. 188, 141–165.
Kowalski, E.A., Dilcher, D.L., 2003. Warmer paleotemperatures for terrestrial ecosystems. Proceedings of the National Academy of Sciences, USA 100, 167–170.
Lau, K.M., Chan, P.H., 1983. Short-term climate variability and atmospheric teleconnections from satellite-observed outgoing longwave radiation. Part I: simultaneous relationships. J. Atmos. Sci. 40 (12), 2751–2767.
Li, Y.Q., Wang, Z.H., Xu, X.T., Han, W.X., Wang, Q.G., Zou, D.Y., 2016. Leaf margin analysis of Chinese woody plants and the constraints on its application to palaeoclimatic reconstruction. Glob. Ecol. Biogeogr. 25 (12), 1401–1415.
Lielke, K., Manchester, S., Meyer, H., 2012. Reconstructing the environment of the northern Rocky Mountains during the Eocene/Oligocene transition: constraints from the palaeobotany and geology of south-western Montana, USA. Acta Palaeobotanica 52 (2), 317–358.
Lowe, A.J., Greenwood, D.R., West, C.K., Galloway, J.M., Markus, S., Tammo, R., 2018. Plant community ecology and climate on an upland volcanic landscape during the Early Eocene Climatic Optimum: McAbee Fossil Beds, British Columbia, Canada. Palaeogeogr. Palaeoclimatol. Palaeoecol. 511, 433–448.
Malhado, A.C.M., Whittaker, R.J., Malhi, Y., Ladle, R.J., ter Steege, H., Butt, N., Aragão, L.E.O.C., Quesada, C.A., Murakami-Araujo, A., Phillips, O.L., Peacock, J., López-González, G., Baker, T.R., Anderson, L.O., Arroyo, L., Almeida, S., Higuchi, N., Killeen, T.J., Monteagudo, A., Neill, D.A., Pitman, N.C.A., Prieto, A., Salomão, R.P., Vásquez-M, R., Laurance, W.F., Ramírez, A.H., 2009. Spatial distribution and functional significance of leaf lamina shape in Amazonian forest trees. Biogeosciences 6, 1577–1590.
Miller, I.M., Brandon, M.T., Hickey, L.J., 2006. Using leaf margin analysis to estimate Mid-Cretaceous (Albian) paleolatitude of the Baja BC block. Earth Planet. Sci. Lett. 245, 95–114.
Mosbrugger, V., Favre, A., Muellner-Riehl, A.N., Päckert, M., Mulch, A., 2018. Cenozoic evolution of geobiodiversity in the Tibeto-Himalayan region. In: Hoorn, C., Perrigo, A., Antonelli, A. (Eds.), Mountains, Climate and Biodiversity. Wiley Blackwell, Oxford, pp. 429–448.
O'Brien, E.M., 2006. Biological relativity to water-energy dynamics. J. Biogeogr. 33 (11), 1868–1888.
Peppe, D.J., Royer, D.L., Cariglino, B., Oliver, S.Y., Newman, S., Leight, E., Enikolopov, G., Fernandez-Burgos, M., Herrera, F., Adams, J.M., Correa, E., Currano, E.D., Erickson, J.M., Hinojosa, L.F., Hoganson, J.W., Iglesias, A., Jaramillo, C.A., Johnson, K.R., Jordan, G.J., Kraft, N.J.B., Lovelock, E.C., Lusk, C.H., Niinemets, Ü., Peñuelas, J., Rapson, G., Wing, S.L., Wright, I.J., 2011. Sensitivity of leaf size and shape to climate: global patterns and paleoclimatic applications. New Phytol. 190, 724–739.
Royer, D.L., Wilf, P., 2006. Why do toothed leaves correlate with cold climates? Gas-exchange at leaf margins provides new insights into a classic paleotemperature proxy. Int. J. Plant Sci. 167 (1), 11–18.
Royer, D.L., Wilf, P., Janesko, D.A., Kowalski, E.A., Dilcher, D.L., 2005. Correlations of climate and plant ecology to leaf size and shape: potential proxies for the fossil record. Am. J. Bot. 92 (7), 1141–1151.
Royer, D.L., McElwain, J.C., Adams, J.M., Wilf, P., 2008. Sensitivity of leaf size and shape to climate within *Acer rubrum* and *Quercus kelloggii*. New Phytol. 179 (3), 808–817.
Royer, D.L., Peppe, D.J., Wheeler, E.A., Niinemets, Ü., 2012. Roles of climate and functional traits in controlling toothed vs. untoothed leaf margins. Am. J. Bot. 99, 915–922.
Shukla, A., Mehrotra, N.C., Spicer, R.A., Spicer, T.E.V., Kumar, M., 2014. Cool equatorial terrestrial temperatures and the South Asian monsoon in the Early Eocene: evidence from the Gurha Mine, Rajasthan, India. Palaeogeogr. Palaeoclimatol. Palaeoecol. 412, 187–198.
Spicer, R.A., 2007. Recent and future developments of CLAMP: building on the legacy of Jack A. Wolfe. CFS Courier Forschungsinstitut Senckenberg 258, 109–118.
Spicer, R.A., 2009. CLAMP, Climate Leaf Analysis Multivariate Program. The Open University(URL http://www.open.ac.uk/earth-research/spicer/CLAMP/Clampset1.html and http://clamp.ibcas.ac.cn/ [last accessed 1 November 2010]).
Spicer, R.A., 2016. CLAMP, Climate Leaf Analysis Multivariate Program. The Open University.
Spicer, R.A., 2017. Tibet, the Himalaya, Asian monsoons and biodiversity–in what ways are they related? Plant Diversity 39, 233–244.
Spicer, R.A., Herman, A.B., Kennedy, E.M., 2004. Foliar physiognomic record of climatic conditions during dormancy: climate Leaf Analysis Multivariate Program (CLAMP) and the cold month mean temperature. J. Geol. 112, 685–702.
Spicer, R.A., Herman, A.B., Kennedy, E.M., 2005. The sensitivity of CLAMP to taphonomic loss of foliar physiognomic characters. Palaios 20, 429–438.
Spicer, R.A., Herman, A.B., Liao, W., Spicer, T.E.V., Kodrul, T.M., Yang, J., Jin, J.H., 2014. Cool tropics in the Middle Eocene: evidence from the Changchang Flora, Hainan Island, China. Palaeogeogr. Palaeoclimatol. Palaeoecol. 412, 1–16.
Spicer, R.A., Yang, J., Herman, A.B., Kodrul, T., Maslova, N., Spicer, T.E.V., Aleksandrova, G., Jin, J.H., 2016. Asian Eocene monsoons as revealed by leaf architectural signatures. Earth Planet. Sci. Lett. 449, 61–68.
Spicer, R.A., Yang, J., Herman, A.B., Kodrul, T., Aleksandrova, G., Maslova, N., Spicer, T.E.V., Ding, L., Xu, Q., Shukla, A., Srivastava, G., Mehrotra, R.C., Jin, J.H., 2017. Paleogene monsoons across India and South China: drivers of biotic change. Gondwana Res. 49, 350–363.
Srivastava, G., Spicer, R.A., Spicer, T.E.V., Yang, J., Kumar, M., Mehrotra, R., Mehrotra, N., 2012. Megaflora and palaeoclimate of a Late Oligocene tropical delta, Makum Coalfield, Assam: evidence for the early development of the South Asia Monsoon. Palaeogeogr. Palaeoclimatol. Palaeoecol. 342–343, 130–142.
Steart, D.C., Spicer, R.A., Bamford, M.K., 2010. Is Southern Africa different? An investigation of the relationship between leaf physiognomy and climate in Southern African mesic vegetation. Rev. Palaeobot. Palynol. 162, 607–620.
Stephenson, N.L., 1990. Climatic control of vegetation distribution: the role of the water balance. Am. Nat. 135, 649–670.
Stranks, L., England, P., 1997. The use of a resemblance function in the measurement of climatic parameters from the physiognomy of woody dicotyledons. Palaeogeogr. Palaeoclimatol. Palaeoecol. 131, 15–28.
Su, T., Xing, Y.W., Liu, Y.S., Jacques, F.M.B., Chen, W.Y., Huang, Y.J., Zhou, Z.K., 2010. Leaf margin analysis: a new equation from humid to mesic forests in China. Palaios 25, 234–238.
Su, T., Spicer, R.A., Liu, Y.S., Huang, Y.J., Xing, Y.W., Jacques, F.M.B., Chen, W.Y., Zhou, Z.K., 2013. Regional constraints on leaf physiognomy and precipitation regression models: a case study from China. Bulletin of Geosicences 88 (3), 595–608.
Sunderlin, D., Loope, G., Parker, N.E., Williams, C.J., 2011. Paleoclimatic and paleoecological implications of a Paleocene-Eocene fossil leaf assemblage, Chickaloon Formation, Alaska. Palaios 26, 335–345.
Tomsich, C.S., McCarthy, P.J., Fowell, S.J., Sunderlin, D., 2010. Paleofloristic and paleoenvironmental information from a Late Cretaceous (Maastrichtian) flora of the lower Cantwell Formation near Sable Mountain, Denali National Park, Alaska. Palaeogeogr. Palaeoclimatol. Palaeoecol. 295, 389–408.
Traiser, C., Klotz, S., Uhl, D., Mosbrugger, V., 2005. Environmental signals from leaves - a physiognomic analysis of European vegetation. New Phytol. 166, 465–484.
Traiser, C., Uhl, D., Klotz, S., Mosbrugger, V., 2007. Leaf physiognomy and palaeoenvironmental estimates-an alternative technique based on an European calibration. Acta Palaeobotanica 47, 183–201.
Uhl, D., Traiser, C., Griesser, U., Denk, T., 2007. Fossil leaves as palaeoclimate proxies in the Palaeogene of Spitsbergen (Svalbard). Acta Palaeobotanica 47, 89–107.
Wang, B., Ho, L., 2002. Rainy season of the Asian-Pacific summer monsoon. J. Clim. 15 (4), 386–398.
Wang, B., Trenberth, K., Hurrell, J., Stepaniak, D., 2006. The Asian Monsoon. Springer, Berlin Heidelberg.
West, C.K., Greenwood, D.R., Basinger, J.F., 2015. Was the Arctic Eocene 'rainforest' monsoonal? Estimates of seasonal precipitation from early Eocene megafloras from Ellesmere Island, Nunavut. Earth Planet. Sci. Lett. 427, 18–30.
Wiemann, M.C., Manchester, S.R., Dilcher, D.L., Hinojosa, L.F., Wheeler, E.A., 1998. Estimation of temperature and precipitation from morphological characters of dicotyledonous leaves. Am. J. Bot. 85, 1796–1802.
Wilf, P., 1997. When are leaves good thermometers? A new case for leaf margin analysis. Paleobiology 23, 373–390.
Wilf, P., Wing, S.L., Greenwood, D.R., Greenwood, C.L., 1998. Using fossil leaves as paleoprecipitation indicators: an Eocene example. Geology 26, 203–206.
Wing, S.L., Greenwood, D.R., 1993. Fossils and fossil climate: the case for equable continental interiors in the Eocene. Philosophical transactions of the Royal Society of London, Series B: Biological Sciences 341, 243–252.
Wolfe, J.A., 1971. Tertiary climatic fluctuations and methods of analysis of Tertiary floras. Palaeogeogr. Palaeoclimatol. Palaeoecol. 9, 27–57.
Wolfe, J.A., 1979. Temperature parameters of humid to mesic forests of eastern Asia and relation to forests of other regions in the Northern Hemisphere and Australasia. U. S. Geol. Surv. Prof. Pap. 1106, 1–37.
Wolfe, J.A., 1993. A method of obtaining climatic parameters from leaf assemblages. United States Geological Survey Bulletin 2040, 1–71.
Wolfe, J.A., Spicer, R.A., 1999. Fossil leaf character states: multivariate analysis. In: Jones, T.P., Rowe, N.P. (Eds.), Fossil Plants and Spores: Modern Techniques Geological Society, London, pp. 233–239.
Woodward, F.I., Lomas, M.R., Kelly, C.K., 2004. Global climate and the distribution of plant biomes. Philosophical Transactions of the Royal Society B: Biological Sciences 359, 1465–1476.

Wright, I.J., Dong, N., Maire, V., Prentice, I.C., Westoby, M., Díaz, S., Gallagher, R.V., Jacobs, B.F., Kooyman, R., Law, E.A., Leishman, M.R., Niinemets, Ü., Reich, P.B., Sack, L., Villar, R., 12 Han Wang, H., Wilf, P., 2017. Global climatic drivers of leaf size. Science 357, 917–921.

Wu, Z.Y. (Ed.), 1979, 1980, 1982, 1984, 1988, 1995, 1996, 1998. Flora of China. vols. 20–72 Science Press, Beijing (In Chinese).

Wu, Z.Y. (Ed.), 1980. Vegetation of China. Science Press, Beijing, pp. 363–397 (In Chinese).

Wu, Z.Y., Ding, T.Y., 1999. Seed Plants of China. Yunnan Science and Technology Press, Kunming (In Chinese).

Xing, Y.W., Utescher, T., Jacques, F.M.B., Su, T., Liu, Y.S., Huang, Y.J., Zhou, Z.K., 2012. Paleoclimatic estimation reveals a weak winter monsoon in southwestern China during the late Miocene: evidence from plant macrofossils. Palaeogeogr. Palaeoclimatol. Palaeoecol. 358–360, 19–26.

Yang, J., Spicer, R.A., Spicer, T.E., Arens, N.C., Jacques, F.M.B., Su, T., Kennedy, E.M., Herman, A.B., Steart, D.C., Srivastava, G., 2015. Leaf form-climate relationships on the global stage: an ensemble of characters. Glob. Ecol. Biogeogr. 24, 1113–1125.

Zhang, J.C., 1991. Climate in China: The Pandect. China Meteorological Press, Beijing, pp. 477 (In Chinese).